Multiplier-Free Intrachannel Nonlinearity Compensating Algorithm Operating at Symbol Rate

Zhenning Tao, *Senior Member, IEEE*, Liang Dou, Weizhen Yan, Lei Li, Takeshi Hoshida, *Member, IEEE*, and Jens C. Rasmussen, *Member, IEEE*

***Abstract*—Intrachannel nonlinearity is considered a major distortion in high-capacity transmission systems particular for the case without inline optical chromatic dispersion compensation. In this paper, a low-complexity intrachannel nonlinear compensator operating at the symbol rate is proposed based on the nonlinear perturbation predistortion for the dual-polarization quadrature phase-shift keying (DP-QPSK) systems. Compared with the widely studied backpropagation algorithm, the proposed algorithm achieves comparable performance with significantly reduced complexity and halved sampling speed in digital signal processing and digital-to-analog converters. The proposed algorithm is demonstrated in a 43 Gb/s DP-QPSK transmission experiment over 1500 km. In addition to the experimental demonstration, numerical simulation verifies that the proposed algorithm is quite robust by tolerating significant uncertainties of link parameters and span-by-span inhomogeneity in the links.**

***Index Terms*—Intrachannel nonlinearity, perturbation, predistortion, quadrature phase-shift keying (QPSK).**

I. Introduction

THE COHERENT detection assisted by digital signal processing is believed to be a major technology for high-capacity long-haul transmission. Since linear distortions such as chromatic dispersion (CD) and polarization-mode dispersion (PMD) can be compensated by a linear equalizer in the receiver [1], the nonlinearities are expected to be the major remaining obstacle [2]. The interchannel nonlinearity can be mitigated either by the transmission link design or by receiver algorithms [3]–[7]. The intrachannel nonlinearity is another major nonlinear distortion. Owning to the deterministic nature of the intrachannel nonlinearity, various compensation algorithms implemented at the receiver and at the transmitter have been proposed.

The most widely studied algorithm is the backpropagation at the receiver [8]–[11]. In dual-polarization (DP) systems, the interaction between the two polarization tributaries should be considered and the backpropagation should be modified accordingly [12]. In order to reduce the complexity of conventional backpropagation, a low-pass filter can be inserted before self-phase modulation compensation [13], or the correlated backpropagation [14] that correlates the signal powers in time domain to determine the amount of self-phase modulation compensation can be used. With these two approaches, the stages of backpropagation can be significantly less than the span number of the link. As a different approach, nonlinear equalizer based on Volterra expansion was proposed in [15] to adaptively mitigate the intrachannel nonlinearity. However, its computational complexity is even higher than that of backpropagation.

Besides the compensation algorithms at the receiver, the predistortion algorithms that transmit the properly distorted waveform and obtain the undistorted waveform after transmission have been proposed [16]–[19]. The properly distorted waveform can be calculated either by the backpropagation algorithm [18] or it can be stored in a lookup table (LUT) [19]. However, the former approach has high complexity and the latter one requires a large size that increases exponentially with the link memory length determined by the CD. For instance, the transmission over 1500 km standard single-mode fiber (SSMF) has 22 000 ps/nm CD that causes to 134 symbol pulse broadening for the 112 Gb/s DP quadrature phase-shift keying (QPSK) modulation format. Consequently, a complete LUT should have a size of 16^{134}.

The major drawback of the current intrachannel nonlinearity compensation method is its high computational complexity. In [20], we demonstrated a multiplier-free predistortion method to compensate the intrachannel nonlinearity, whereas the performance is comparable with the backpropagation. In this paper, we explain the detailed theory behind the proposed method that was omitted in [20]. The other important aspect that was not discussed in [20] is the robustness of this technique against link parameter uncertainties. Since predistortion requires the system information to calculate the properly distorted waveform, a natural argument is "how many uncertainties of link parameters can be tolerated." In this paper, numerical simulation results are presented to address this issue.

This paper is organized as follows. In Section II, we provide the theory of predistortion algorithm based on perturbation analysis. In Section III, the proposed algorithm is demonstrated in a 43 Gb/s DP-QPSK experiment. In Section IV, the tolerance to the link parameter uncertainties is investigated by simulation.

II. Theory of the Predistortion Algorithm

A. Perturbation Analysis of Manakov Equations

In this section, we illustrate the perturbation analysis of DP transmission that is the foundation of the proposed predistortion algorithm.

Manuscript received April 19, 2011; revised June 16, 2011; accepted June 18, 2011. Date of publication June 30, 2011; date of current version August 17, 2011.

Z. Tao, L. Dou, W. Yan, and L. Li are with the Fujitsu R&D Center, Beijing 100025, China (e-mail: taozn@cn.fujitsu.com; douliang@cn.fujitsu.com; yanwz@cn.fujitsu.com; lilei@cn.fujitsu.com).

T. Hoshida and J. C. Rasmussen are with Fujitsu Laboratories, Ltd., Kawasaki 211-8588, Japan (e-mail: hoshida@jp.fujitsu.com; jens.rasmussen@jp.fujitsu.com).

Color versions of one or more of the figures in this paper are available online at http://ieeexplore.ieee.org.

Digital Object Identifier 10.1109/JLT.2011.2160933

At first, the perturbation analysis of single-polarization transmission proposed by Mecozzi *et al.* [21] is reviewed. The nonlinear Schrödinger equation is

$$\frac{\partial}{\partial z}u(t,z)+j\frac{\beta_2}{2}\frac{\partial^2}{\partial t^2}u(t,z)=j\gamma|u(t,z)|^2u(t,z) \quad (1)$$

where $u(t,z)$ is the optical field, β_2 is the group velocity dispersion, and γ is the nonlinear coefficient. Hereafter, the nonlinear term in (1) is treated as perturbing by denoting $u(t,z)=u_0(t,z)+\Delta u(t,z)$, where $u_0(t,z)$ is the solution of linear propagation and $\Delta u(t,z)$ is the perturbation due to the nonlinear effects. Assuming the input signal as Gaussian pulse train, the three input pulses $A_0\exp(-(t-T_{m/l/n})^2/2\tau^2)$ at time T_m,T_l,T_n generates a ghost pulse

$$\begin{aligned}\Delta u(t+T_m-T_l+T_n,L)&=j\gamma A_0^3\exp\left(\frac{-t^2}{6\tau^2}\right)\\&\quad\times\int_0^L dz\frac{1}{\sqrt{1+2j\beta_2z/\tau^2+3(\beta_2z/\tau^2)^2}}\\&\quad\times\exp\left\{\begin{array}{l}-\frac{3[2t/3+T_m-T_l][2t/3+T_n-T_l]}{\tau^2(1+3j\beta_2z/\tau^2)}\\-\frac{(T_n-T_m)^2}{\tau^2[1+2j\beta_2z/\tau^2+3(\beta_2z/\tau^2)^2]}\end{array}\right\}.\end{aligned} \quad (2)$$

Then, we extend the perturbation analysis to the DP transmission by considering the Manakov equation that describes the optical field evolution through the fiber links where the nonlinear effective length is much longer than the fiber birefringent beating length [22]

$$\begin{aligned}&\frac{\partial}{\partial z}u_x(t,z)+j\frac{\beta_2}{2}\frac{\partial^2}{\partial t^2}u_x(t,z)\\&\quad=j\frac{8}{9}\gamma[|u_x(t,z)|^2+|u_y(t,z)|^2]u_x(t,z) \quad (3)\\&\frac{\partial}{\partial z}u_y(t,z)+j\frac{\beta_2}{2}\frac{\partial^2}{\partial t^2}u_y(t,z)\\&\quad=j\frac{8}{9}\gamma[|u_x(t,z)|^2+|u_y(t,z)|^2]u_y(t,z) \quad (4)\end{aligned}$$

where $u_{x/y}(t,z)$ is the optical field of *x* and *y* polarizations, respectively. The perturbations $\Delta u_{x/y}(t,z)$ should satisfy

$$\begin{aligned}&\frac{\partial}{\partial z}\Delta u_{x/y}+j\frac{\beta_2}{2}\frac{\partial^2}{\partial t^2}\Delta u_{x/y}\\&\qquad=j\frac{8\gamma}{9}[|u_{x/y,0}|^2+|u_{y/x,0}|^2]u_{x/y,0}\end{aligned} \quad (5)$$

where $u_{x/y,0}$ is the solution to linear propagation. In (5), explicit dependence on z and t was omitted for compactness. The Fourier transform of (5), by taking *x* polarization as an example, is

$$\frac{\partial}{\partial z}\Delta\tilde{u}_x(\omega,z)-j\frac{\omega^2\beta_2}{2}\Delta\tilde{u}_x(\omega,z)=\tilde{F}_x(\omega,z) \quad (6)$$

where $\tilde{F}(\omega,z)$ is the Fourier transform of the right side of (5), i.e.,

$$\begin{aligned}\tilde{F}_x(\omega,z)=j\frac{8\gamma}{9}\left[\int e^{-j\omega t}u_{x,0}u_{x,0}^*u_{x,0}dt\right.\\\left.+\int e^{-j\omega t}u_{y,0}u_{y,0}^*u_{x,0}dt\right].\end{aligned} \quad (7)$$

Equation (6) is an inhomogeneous linear differential equation having a variable z and a parameter ω. After solving (6), the frequency-domain perturbation at $z=L$ is found to be

$$\begin{aligned}\Delta\tilde{u}_x(\omega,L)&=\exp(j\omega^2\beta_2L/2)\\&\quad\times\int_0^L\tilde{F}_x(\omega,z)\exp(-j\omega^2\beta_2z/2)dz.\end{aligned} \quad (8)$$

The time-domain nonlinear perturbation is obtained by processing the inverse Fourier transform on both sides of (8). If we compare it with the single-polarization transmission case, there is an additional term $\int e^{-j\omega t}u_{y,0}u_{y,0}^*u_{x,0}dt$ in $\tilde{F}_x(\omega,z)$. This new term corresponds to nonlinear interaction between the two polarization tributaries.

Through the same procedure as that of [21], the time-domain nonlinear perturbation can be solved analytically. The six input Gaussian pulses $\sqrt{P_0}A_{m/l/n,x/y}\exp(-(t-T_{m/n/l})^2/2\tau^2)$ at three timings T_m,T_l,T_n for the two polarizations generate the ghost pulse on *x* polarization as follows:

$$\begin{aligned}\Delta u_x(t+T_m-T_l+T_n,L)&=j\frac{8}{9}\gamma P_0^{3/2}[A_{n,x}A_{l,x}^*A_{m,x}+A_{n,y}A_{l,y}^*A_{m,x}]\\&\quad\times\exp\left(\frac{-t^2}{6\tau^2}\right)\\&\quad\times\int_0^L dz\frac{1}{\sqrt{1+2j\beta_2z/\tau^2+3(\beta_2z/\tau^2)^2}}\\&\quad\times\exp\left\{\begin{array}{l}-\frac{3[2t/3+T_m-T_l][2t/3+T_n-T_l]}{\tau^2(1+3j\beta_2z/\tau^2)}\\-\frac{(T_n-T_m)^2}{\tau^2[1+2j\beta_2z/\tau^2+3(\beta_2z/\tau^2)^2]}\end{array}\right\}\end{aligned} \quad (9)$$

where P_0 is the pulse peak power and $A_{m/l/n,x/y}$ is extended to an arbitrary complex value. The additional term with a factor $A_{n,y}A_{l,y}^*A_{m,x}$ in (9) is attributed to the nonlinear interaction between the *x* and *y* polarizations originating from the term $\int e^{-j\omega t}u_{y,0}u_{y,0}^*u_{x,0}dt$ in (7). The perturbation of *y* polarization $\Delta u_y(t+T_m-T_l+T_n,L)$ is obtained by simply exchanging the subscripts *x* and *y*.

B. Predistortion Algorithm

The basic idea of the proposed algorithm is to calculate the perturbation caused by intrachannel nonlinearity firstly, and then to subtract the perturbation to generate the predistorted waveform. In this section, the predistortion algorithm for DP systems is illustrated.

Without losing generality, in the following, we focus on the perturbation of the symbol with index of 0, i.e., $l=m+n$. Since the predistortion is assumed to operate at the symbol rate, only the perturbation value at $t=0$ is considered. In typical high-capacity transmission systems, in particular the ones without in-line CD compensation, the pulse spreading due to CD is usually much larger than the symbol duration (i.e., $\beta_2z\gg\tau^2$). With this

large CD assumption, the perturbation for the zeroth symbol at $t = 0$ by (9) is simplified as

$$\Delta u_x = \sum_{m,n} P_0^{3/2}(A_{n,x}A_{m+n,x}^* A_{m,x} + A_{n,y}A_{m+n,y}^* A_{m,x})C_{m,n} \quad (10a)$$

$$\Delta u_y = \sum_{m,n} P_0^{3/2}(A_{n,y}A_{m+n,y}^* A_{m,y} + A_{n,x}A_{m+n,x}^* A_{m,y})C_{m,n} \quad (10b)$$

where P_0 is the pulse peak power at the launch point. $A_{m/l/n,x/y}$ is the symbol complex amplitude imposed by data modulation. The nonlinear perturbation coefficient $C_{m,n}$ is given by

$$C_{m,n} = j\frac{8}{9}\frac{\gamma\tau^2}{\sqrt{3}|\beta_2|}E_1\left(-j\frac{mnT^2}{\beta_2 L}\right) \quad m \neq 0, n \neq 0 \quad (11a)$$

$$C_{m,n} = j\frac{8}{9}\frac{\gamma\tau^2}{\sqrt{3}|\beta_2|}\frac{1}{2}E_1\left(\frac{(n-m)^2T^2\tau^2}{3|\beta_2|^2L^2}\right) \quad m \text{ or } n = 0 \quad (11b)$$

$$C_{0,0} = j\frac{8}{9}\frac{\gamma\tau^2}{\sqrt{3}|\beta_2|}\int_0^L dz \frac{1}{\sqrt{\tau^4/(3\beta_2^2) + z^2}} \quad (11c)$$

where τ, T, and L are, respectively, the pulsewidth, the inverse of symbol rate, and the transmission distance, m/n is the symbol indexes, and $E_1(\cdot)$ is the exponential integral function [23]. Equation (11a) represents the coefficients of the intrachannel four-wave mixing (IFWM) terms and (11b) shows the intrachannel cross-phase modulation (IXPM) terms [24]. In the derivation of (9) and (11), the fiber attenuation is ignored. However, the real transmission link has fiber attenuation and inline optical amplifiers. To accommodate such a real link, the nonlinear perturbation coefficient is scaled by a factor $L_{\text{eff}}/L_{\text{span}}$, where L_{eff} is the effective length of each span and L_{span} is the span length.

It is noteworthy that the transmitted data $A_{m/n,x/y}$ can be any arbitrary complex values so that the perturbation calculation of (10) is compatible with various modulation formats including ON–OFF keying, m-ary phase-shift keying (mPSK), and quadrature amplitude modulation as long as the pulse spreading caused by CD is much larger than the symbol duration. In the following, we narrow it down to the DP-QPSK modulated system without optical inline CD compensation mainly because it is the major trend of the optical communication system design at or beyond 100 Gb/s.

At first, we consider the predistortion for the IXPM term where m or n equals 0. The perturbation contribution of IXPM is

$$\Delta u_x^{\text{IXPM}} = P_0^{3/2}\sum_m A_{0,y}A_{m,y}^* A_{m,x}C_{m,0} + P_0^{3/2}A_{0,x} \times \left[\sum_n (|A_{n,x}|^2 + |A_{n,y}|^2)C_{0,n} + \sum_{m\neq 0}|A_{m,x}|^2 C_{m,0}\right]. \quad (12)$$

In the case of mPSK modulation, the modulus $|A_{m/n,x/y}|^2$ is always constant (assumed to be unity in the following), so the second term in (12) does not depend on the symbol pattern. Considering that $C_{m,n}$ is a pure imaginary number for m or $n = 0$, the perturbation of the second term just results in a constant phase rotation and thus can be compensated by the carrier phase recovery in the receiver. As a consequence, only the term of the first line, which depends on the symbol pattern and is time varying and, therefore, should be included in the predistortion. It is noteworthy that no predistortion was required for compensating IXPM in single-polarization mPSK modulation because of the absence of the first line of (12).

Second, the perturbation contribution of IFWM $\sum_{m\neq 0,n\neq 0} P_0^{3/2}(A_{n,x}A_{m+n,x}^* A_{m,x} + A_{n,y}A_{m+n,y}^* A_{m,x})C_{m,n}$ is always symbol pattern dependent and should be considered in the predistortion. The second term in the bracket indicates the nonlinear interplay between the two polarization tributaries; therefore, the predistortion should also include two polarizations.

After analyzing the perturbation of IXPM and IFWM, the predistortion for DP-QPSK system is

$$\Delta u_x = P_0^{3/2}\left[\sum_{m\neq 0,n\neq 0} A_{n,x}A_{m+n,x}^* A_{m,x}C_{m,n} + \sum_{m\neq 0,n} A_{n,y}A_{m+n,y}^* A_{m,x}C_{m,n}\right] \quad (13)$$

where $C_{m,n}$ is given by (11) and $A_{m/n,x/y}$ is the symbol complex amplitude. The predistortion for *y* polarization is obtained by simply exchanging the subscripts *x* and *y*.

C. Complexity of the Predistortion Algorithm

Equation (13) includes a 2-D summation of three product terms and looks fairly complex. However, its implementation can be noticeably simple for the DP-QPSK modulation format because of three reasons. At first, The coefficient $C_{m,n}$ depends just on the link configuration and can be stored in a quasi-static LUT after offline calculation. Second, the product of any QPSK symbols is always a QPSK symbol, so the multiplication of QPSK symbols can be implemented by simple logical operation. Furthermore, because the QPSK symbol can be represented as one of $1, -1, j$, and $-j$, the multiplication between the QPSK symbol and the coefficient $C_{m,n}$ is also replaceable by logical operations, e.g., swapping of real and imaginary parts or polarity inversion of the real or imaginary part. As a result, the bracket in (13) can be implemented by simple logical operations and adders. The complexity of such implementation is governed by the number of summation terms used in (13). Third, the predistortion does not require oversampling in the digital signal processing or in the digital-to-analog converter (DAC), so the requirement on the circuit is significantly relaxed.

As a summary of Section II, the block diagram of the DP-QPSK transmitter with the proposed intrachannel nonlinearity compensator is shown in Fig. 1, where the perturbation calculation is given by (13) and the coefficient $C_{m,n}$ is given by (11).

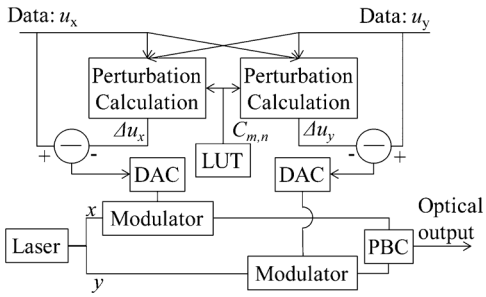

Fig. 1. Block diagram of the DP-QPSK transmitter equipped with the proposed intrachannel nonlinearity compensator. PBC: polarization beam combiner, DAC: digital-to-analog converter, LUT: look up table that contains the nonlinear perturbation coefficient $C_{m,n}$.

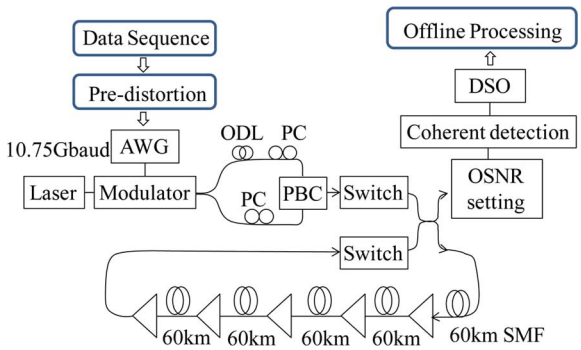

Fig. 2. Experimental setup. AWG: arbitrary waveform generator. PC: polarization controller. ODL: optical delay line with half PRBS period delay. PBC: polarization beam combiner. SSMF: standard single-mode fiber. DSO: digital storage oscilloscope.

III. Experimental Verification

A. Experimental Setup and Methodology

In order to evaluate the performance of the proposed predistortion algorithm, a single channel 43 Gb/s DP return-to-zero (RZ) QPSK transmission experiment with coherent detection was carried out. The symbol-aligned RZ format was chosen mainly because the perturbation theory assumes Gaussian pulse that also returns to zero at the symbol edge. The improvement by predistortion for nonreturn-to-zero format is expected to be less than RZ format.

Fig. 2 shows the experimental setup. The fiber loop consisted of five spans of 60 km long SSMF and there was no inline dispersion compensation. The transmitter operated on 10.75 Gbaud due to the limitation of the arbitrary waveform generator (AWG). The major ASE noise was loaded at receiver and the optical signal-to-noise ratio (OSNR) was adjusted accordingly. At the receiver, the optical field waveform was captured by the digital storage oscilloscope having a sample rate of 50 GSa/s. Then, offline processing in a personal computer that included sampling rate conversion to 2 samples per symbol, static CD compensation, a 11-tap adaptive equalizer driven by constant modulus algorithm, laser frequency offset compensation, and Viterbi–Viterbi carrier phase recovery with optimized sliding average window was carried out.

In general, four-channel DACs are required in the experiment because there is nonlinear interaction between x and y polarization and the perturbations of x and y polarization are, therefore, not equal. In order to carry out the experiment with the available AWG that only has two DAC channels, we carefully selected the length of optical delay line to be exactly half of the random sequence period that was 2^{13} symbols. By this way, the perturbations in each polarization were the same except for a half-period delay, and the information data of each polarization were also the same except for a half-period delay.

The perturbation calculation equation (13) contains infinite terms when m, n approaches infinite. In the experiment, we truncated them when the coefficient $C_{m,n}$ was less than a threshold. The default threshold was defined so that the magnitude of $C_{m,n}$ was 1/100 of the maximum magnitude (that of $C_{0,0}$) and the corresponding number of $C_{m,n}$ terms was 1413. The impact of threshold selection was also investigated later.

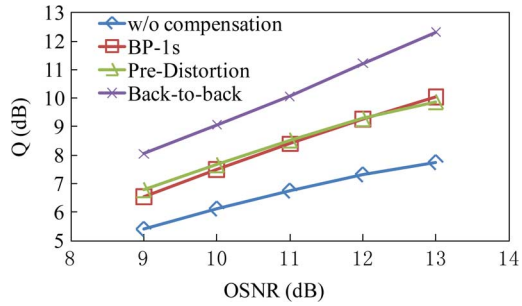

Fig. 3. Performance comparison between the proposed predistortion method (triangles) and backpropagation having one stage per span (BP-1s, squares) after 25 × 60 km transmission with 2 dB·m launch power.

B. Performance of the Proposed Predistortion Algorithm

The performance of the proposed predistortion algorithm is shown and compared with the widely studied backpropagation compensator that employs one stage per span in this section. To evaluate the system performance, we adopted the Q value that is defined as $Q_{\mathrm{dB}} = 20\log_{10}(\sqrt{2}erfc^{-1}(2\mathrm{BER}))$, where $erfc^{-1}(\cdot)$ is the inverse complementary error function and the BER is bit-error ratio measured by counting bit errors within more than 10^6 symbols.

Fig. 3 shows the Q values as a function of OSNR with 0.1 nm noise bandwidth after 1500 km (25 span) transmission when the time-averaged launch power of each fiber span was 2 dB·m. The pulse peak power P_0 used for predistortion calculation was selected as 5 dB·m so that the time-averaged power after predistortion was still 2 dB·m. The pulsewidth τ used in predistortion calculation was 46.5 ps (half of the symbol period). The back-to-back Q values are also shown as a reference. The intrachannel nonlinear compensator improved the Q value by 2 dB and reduced the nonlinear penalty from 3.9 to 1.9 dB. It is clear that both the predistortion algorithm and the backpropagation had similar performance with a small Q value difference less than 0.2 dB.

Fig. 4 shows the performance comparison at different launch powers with a fixed OSNR of 11 dB. The back-to-back Q at 11 dB OSNR is 10.1 dB. The proposed predistortion method showed comparable performance as backpropagation throughout the launch power range between 0 and 3 dB·m. The Q difference is less than 0.1 dB except for 3 dB·m launch power, where the Q value of predistortion is 0.5 dB lower. This

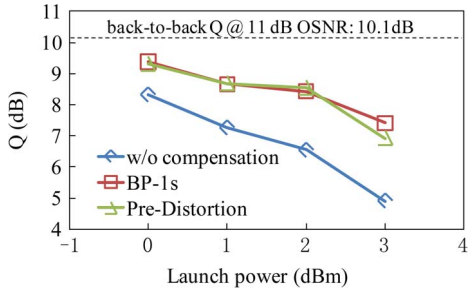

Fig. 4. Launch power dependency of Q values after 25 × 60 km transmission with a fixed OSNR of 11 dB.

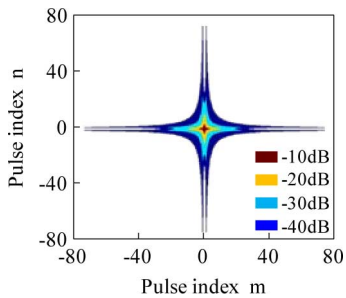

Fig. 5. Example of the magnitude of the coefficient $C_{m,n}$ that is normalized to $C_{0,0}$ (1500 km transmission through SSMF).

degradation at 3 dB·m might be ascribed to the perturbation assumption that the nonlinearity should be small.

C. Performance and Complexity

As shown in (13), the complexity and performance of the predistortion are mainly determined by the number of terms used in the predistortion. In general, as the more terms are used, the higher performance is achieved while the higher complexity is required. The relationship between the performance and the number of terms is shown in this section.

According to (13), the contribution of each perturbation term is mainly determined by the coefficient $C_{m,n}$. Fig. 5 shows an example of the amplitudes of the coefficients $C_{m,n}$ calculated for the link in Fig. 2. Here, $C_{m,n}$ is shown in relative magnitude with respect to the largest one $(C_{0,0})$. The decibel in the figure is defined as $20\log_{10}(|C_{m,n}|/|C_{0,0}|)$. The closest pulses have the largest contribution to the perturbation and the number of terms inside of every 10 dB region grows exponentially. Fig. 6 shows that the Q improvement, defined as the Q value with predistortion minus that without predistortion, increases with the number of terms. The term selection criterion is to discard the terms whose normalized coefficient is less than the threshold. When the cutoff threshold is set to -40 dB, the number of terms is 1413. The boundary of the Q improvement that is defined as the Q of back-to-back minus Q without compensation is also shown as a reference.

IV. Robustness of the Predistortion Algorithm

A. Factors That Might Inhibit Predistortion Performance

The experimental results in Section III demonstrated the proposed predistortion algorithm in a typical laboratory configuration. In reality, however, the system parameters such as CD, span length, and signal power may suffer from fluctuations and

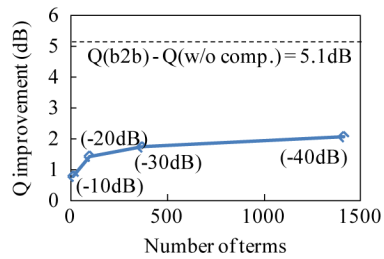

Fig. 6. Q improvement versus number of terms included in the predistortion. Major parameters: 25 × 60 km, 11 dB OSNR and 3 dB·m launch power. Numbers in the brackets show the corresponding cutoff threshold.

uncertainties that could deviate the predistortion performance from the optimum. Numerical simulations in this section, therefore, investigate the tolerance to such uncertainties.

According to (11) and (13), there are following parameters used for perturbation calculation: nonlinear coefficient γ, pulsewidth τ, group velocity dispersion β_2, pulse launch peak power P_0, transmission distance L, symbol duration T, and total CD $\beta_2 L$. These parameters can be divided into two categories. One is the parameters within the exponential integral function $E_1(\,)$ which thereby affects the dependence on symbol index (m,n). The uncertainties of the parameters in this category are mainly relevant to the error in total CD $\beta_2 L$. The other is the parameters outside of the exponential integral function that thereby affects the perturbation amplitude. The uncertainties of the parameters in this category are mainly relevant to the error in nonlinear coefficient γ.

In addition, the deriving process of (11) assumes a homogeneous, periodically amplified link. However, the real link is usually inhomogeneous such as different fiber lengths and launch powers from span to span. The tolerance to such mismatch between the homogenous assumption and inhomogeneous reality is also investigated in this section.

B. Tolerance to the System Parameter Uncertainties

To evaluate the robustness of the proposed predistortion algorithm to the aforementioned uncertainties, we carried out a numerical simulation of single-channel 112 Gb/s DP-QPSK transmission over 1500 km SSMF without inline CD compensation. The ASE noise was loaded at receiver and generated 13.5 dB OSNR that causes Q value limitation of 10 dB. The default system parameters are 25 span with 60 km fiber per span, 3 dB·m launch power, 0.2 dB/km fiber attenuation coefficient, 16 ps/km/nm CD coefficient, and zero PMD. The parameter P_0 used in predistorted waveform calculation was 6 dB·m and the pulsewidth τ was 17.9 ps. At the receiver side, the majority of the accumulated dispersion was compensated optically. The bandwidth of electrical low-pass filter was optimized and set to 19 GHz. BER was achieved by counting the error number (>100) by adding noises with 30 different random seeds for one fixed signal pseudorandom bit sequence (PRBS) pattern having 4096 symbols.

At first, the tolerance to the uncertainty of CD is investigated. In simulation, the CD value used for deriving the predistortion was swept, while the transmission link did not change. Here, the uncertainty is defined as the difference between the value used for predistortion and the actual value divided by the actual value. At receiver, the CD was 100% compensated so that the

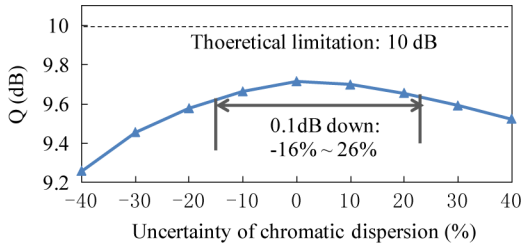

Fig. 7. Tolerance to the uncertainty of CD.

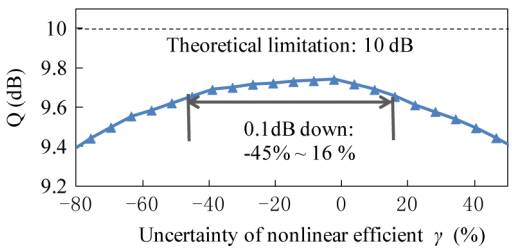

Fig. 8. Tolerance to the uncertainty of nonlinear coefficient.

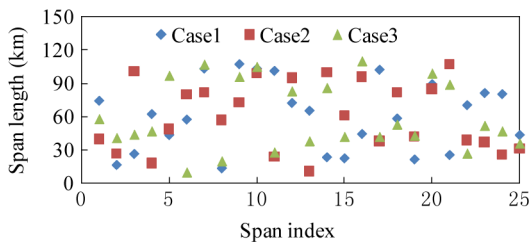

Fig. 9. Representative span length profile of inhomogeneous link.

investigation focused on intrachannel nonlinearity compensation. Fig. 7 shows the Q value as a function of CD uncertainty. Supposing 0.1 dB degradation is allowed, the CD uncertainty range covers -16%–26% that is as large as 42%.

Second, the tolerance to the uncertainty of nonlinear coefficient was investigated in a similar methodology. Fig. 8 shows the 0.1 dB down uncertainty range is as large as -45%–16%. In other words, 61% uncertainty can be tolerated with 0.1 dB Q degradation.

C. Inhomogeneous Span Lengths and Launch Powers

In the calculation of (11) and (13), the link homogeneity is assumed, whereas the real link may be inhomogeneous from span to span. The impact of unequal span lengths and launch powers are shown in this section. As first, we selected ten different inhomogeneous span length profiles whereby the span number was 25 and the total transmission distance was still maintained to be 1500 km. The span lengths were randomly chosen to satisfy uniform distribution in a range from 10 to 110 km. Fig. 9 shows three typical span length profiles.

In spite of such significant difference in span length profiles, the predistortion was conducted using the same perturbation based on homogeneous link assumption. Encouragingly, simulation shows that the predistortion is quite robust against the link profile deviations. Fig. 10 shows the deviation of Q value with predistortion is less than 0.1 dB among the ten span length profiles. This phenomenon indicates intrachannel nonlinearity

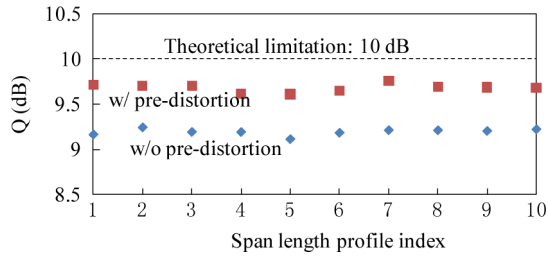

Fig. 10. Q values of ten different span length profiles. Span number: 25; total length: 1500 km; span length uniformly distributed from 10 to 110 km.

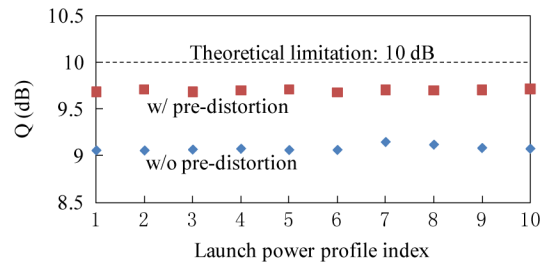

Fig. 11. Q values of ten different launch power profiles. Span number: 25; total length: 1500 km; launch power to each span was randomly in a range from 1.4 to 2.8 mW, keeping the total nonlinear phase shift to be the same.

is less sensitive to the specific span length profile for the inline dispersion compensation-free link. The observation is also supported by the low dependence of Q value without predistortion on the span length profiles.

Second, the fiber launch power may deviate from span to span. To evaluate the impact of such deviation, we selected ten random launch power profiles where the launch powers to each span were uniformly distributed from 1.4 to 2.8 mW. The fiber length in each span was 60 km and total length was 1500 km. For fair comparison, the nonlinear phase shift of each profile was maintained to be the same as the reference configuration where the launch power to every span was 2 mW (3 dB·m) so that the nonlinear distortion of each profile should be the same roughly. Fig. 11 shows the Q values with the ten different launch power profiles. Again, the predistortion turned out to be very robust against the inhomogeneous link.

V. Conclusion

The intrachannel nonlinearity compensation is an essential technology for the next generation of high-capacity transmission systems. A multiplier-free predistortion algorithm operating at the symbol rate has been proposed to compensate the intrachannel nonlinearity for the DP-QPSK systems based on perturbation analysis. Experimental results have proved that it is almost as powerful as the backpropagation method, while it greatly reduces the processing complexity. Various numerical simulations were conducted to demonstrate the robustness of the proposed algorithm to various link parameter uncertainties such as CD, nonlinear coefficient, inhomogeneous span lengths, and random fiber launch powers.

References

[1] E. Ip, A. P. T. Lau, D. J. F. Barros, and J. M. Kahn, "Coherent detection in optical fiber systems," *Opt. Exp.*, vol. 16, no. 2, pp. 753–791, Jan. 2008.

[2] A. Bononi, P. Serena, and N. Rossi, "Nonlinear limits in single- and dual-polarization transmission," presented at the IEEE Photon. Soc. Summer Top. Meeting, Playa del Carmen, Mexico, Jul. 2010, Paper TuA3.3.
[3] Z. Tao, W. Yan, S. Oda, T. Hoshida, and J. C. Rasmussen, "A simplified model for nonlinear cross-phase modulation in hybrid optical coherent system," *Opt. Exp.*, vol. 17, no. 16, pp. 13860–13868, Aug. 2009.
[4] Z. Tao, W. Yan, L. Liu, L. Li, S. Oda, T. Hoshida, and J. C. Rasmussen, "Simple fiber model for determination of XPM effects," *J. Lightw. Technol.*, vol. 29, no. 7, pp. 974–986, Apr. 2011.
[5] L. Li, Z. Tao, L. Liu, W. Yan, S. Oda, T. Hoshida, and J. C. Rasmussen, "XPM tolerant adaptive carrier phase recovery for coherent receiver based on phase noise statistics monitoring," presented at the Eur. Conf. Opt. Commun., Vienna, Austria, Sep. 2009, Paper P3.16.
[6] L. Li, Z. Tao, L. Liu, W. Yan, S. Oda, T. Hoshida, and J. C. Rasmussen, "Nonlinear polarization crosstalk canceller for dual-polarization digital coherent receivers," presented at the Opt. Fiber Commun. Conf./Collocated Natl. Fiber Opt. Eng. Conf., San Diego, CA, Mar. 2010, Paper OWE3.
[7] W. Yan, Z. Tao, L. Li, S. Oda, T. Hoshida, and J. C. Rasmussen, "Multi-stage carrier phase recovery and nonlinear polarization crosstalk canceller for XPM mitigation," presented at the Opt. Fiber Commun. Conf./Collocated Natl. Fiber Opt. Eng. Conf., Los Angeles, CA, Mar. 2011, Paper OWW5.
[8] E. Ip and J. M. Kahn, "Compensation of dispersion and nonlinear impairments using digital backpropagation," *J. Lightw. Technol.*, vol. 26, no. 20, pp. 3416–3425, Oct. 2008.
[9] K. Kikuchi, "Electronic post-compensation for nonlinear phase fluctuations in a 1000-km 20-Gbit/s optical quadrature phase-shift keying transmission system using the digital coherent receiver," *Opt. Exp.*, vol. 16, no. 2, pp. 889–896, Jan. 2008.
[10] X. Li, X. Chen, G. Goldfarb, E. Mateo, I. Kim, F. Yaman, and G. Li, "Electronic post-compensation of WDM transmission impairments using coherent detection and digital signal processing," *Opt. Exp.*, vol. 16, no. 2, pp. 880–888, Jan. 2008.
[11] C. Xie and R. Essiambre, "Electronic nonlinearity compensation in 112-Gb/s PDM-QPSK optical coherent transmission systems," presented at the Eur. Conf. Opt. Commun., Torino, Italy, Sep. 2010, Paper Mo.1.C.1.
[12] S. Oda, T. Tanimura, T. Hoshida, C. Ohshima, H. Nakashima, Z. Tao, and J. C. Rasmussen, "112 Gb/s DP-QPSK transmission using a novel nonlinear compensator in digital coherent receiver," presented at the Opt. Fiber Commun. Conf./Collocated Natl. Fiber Opt. Eng. Conf., San Diego, CA, Mar. 2009, Paper OThR6.
[13] L. B. Du and A. J. Lowery, "Improved single channel backpropagation for intra-channel fiber nonlinearity compensation in long-haul optical communication systems," *Opt. Exp.*, vol. 18, no. 16, pp. 17075–17088, Aug. 2010.
[14] L. Li, Z. Tao, L. Dou, W. Yan, S. Oda, T. Tanimura, T. Hoshida, and J. C. Rasmussen, "Implementation efficient nonlinear equalizer based on correlated digital backpropagation,," presented at the Opt. Fiber Commun. Conf./Collocated Natl. Fiber Opt. Eng. Conf., Los Angeles, CA, Mar. 2011, Paper OWW3.
[15] Y. Gao, F. Zhang, J. Li, L. Liu, Z. Chen, L. Zhu, L. Li, and A. Xu, "Experimental demonstration of nonlinear electrical equalizer to mitigate intra-channel nonlinearities in coherent QPSK systems," presented at the Eur. Conf. Opt. Commun., Vienna, Austria, Sep. 2009, Paper 9.4.7.
[16] L. Dou, Z. Tao, L. Liu, T. Hoshida, and J. C. Rasmussen, "Electronic pre-distortion operating at 1 sample/symbol with accurate bias control for CD compensation," presented at the Opt. Fiber Commun. Conf./Collocated Natl. Fiber Opt. Eng. Conf., San Diego, CA, Mar. 2010, Paper OThT4.
[17] C. Weber, J. K. Fischer, C. A. Bunge, and K. Petermann, "Electronic precompensation of intrachannel nonlinearities at 40 Gb/s," *IEEE Photon. Technol. Lett.*, vol. 18, no. 16, pp. 1759–1761, Aug. 2006.
[18] K. Roberts, C. Li, L. Strawczynski, M. O'Sullivan, and I. Hardcastle, "Electronic precompensation of optical nonlinearity," *IEEE Photon. Technol. Lett.*, vol. 18, no. 2, pp. 403–405, Jan. 2006.
[19] P. J. Winzer and R. J. Essiambre, "Electronic pre-distortion for advanced modulation formats," presented at the Eur. Conf. Opt. Commun., Glasgow, Scotland, Sep. 2005, Paper Tu4.2.2.
[20] L. Dou, Z. Tao, L. Li, W. Yan, T. Tanimura, T. Hoshida, and J. C. Rasmussen, "A low complexity pre-distortion method for intra-channel nonlinearity," presented at the Opt. Fiber Commun. Conf./Collocated Natl. Fiber Opt. Eng. Conf., Los Angeles, CA, Mar. 2011, Paper OThF5.
[21] A. Meccozi, C. B. Clausen, and M. Shtaif, "Analysis of intrachannel nonlinear effects in highly dispersed optical pulse transmission," *IEEE Photon. Technol. Lett.*, vol. 12, no. 4, pp. 392–394, Apr. 2000.
[22] C. R. Menyuk and B. S. Marks, "Interaction of polarization mode dispersion and nonlinearity in optical fiber transmission systems," *J. Lightw. Technol.*, vol. 24, no. 7, pp. 2806–2826, Jul. 2006.
[23] M. Abramowitz and I. A. Stegun, *Handbook of Mathematical Functions*. New York: Dover, 1972.
[24] S. Kumar, J. C. Mauro, S. Raghavan, and D. Q. Chowdhury, "Intrachannel nonlinear penalties in dispersion-managed transmission systems," *IEEE J. Sel. Topics Quantum Electron.*, vol. 8, no. 3, pp. 626–631, May/Jun. 2002.

Zhenning Tao (S'98–M'01–SM'09) received the B.S. degree in physics and the Ph.D. degree in communications and information systems from Peking University, Beijing, China, in 1996 and 2001, respectively.

Since 2001, he has been with Fujitsu R&D Center, Beijing, where he is engaged in research and development of optical fiber communication system and subsystems. His current research interests include optical transmission system, in particular the digital coherent technologies.

Dr. Tao received the Institute of Electronics, Information and Communication Engineers and the Optical Communication Systems Best Paper Awards in 2008 and 2010, and Fujitsu Laboratory President Award in 2010. He is a member of the Optical Society of America.

Liang Dou received the B.S. degree in electronics and the Ph.D. degree in communications and information systems from Peking University, Beijing, China, in 2003 and 2008, respectively.

Since 2008, he has been with Fujitsu R&D Center, Beijing, where he is engaged in research and development of optical fiber communication system and subsystems. His current research interests include optical transmission system, in particular the digital coherent technologies.

Weizhen Yan received the Bachelor's degree in electronics and the M.E. degree in communication and information system from Peking University, Beijing, China, in 2004 and 2007, respectively.

Since 2007, he has been with Fujitsu R&D Center Company Ltd., Beijing, where he has been engaged in the research and development of optical digital coherent technologies.

Lei Li received the Bachelor's degree in information and communication engineering from Xi'an Jiaotong University, Xi'an, China, in 1999, and the Master's degree in electrical engineering from the University of Toledo, Toledo, OH, in 2002.

In 2002, he joined Fujitsu R&D Center Company Ltd., Beijing, China, where he has been engaged in the research and development of optical digital coherent technologies since 2006.

Takeshi Hoshida (S'97–M'98) received the B.E., M.E., and Ph.D. degrees in electronic engineering from the University of Tokyo, Tokyo, Japan, in 1993, 1995, and 1998, respectively.

Since 1998, he has been with Fujitsu Laboratories Ltd., Kawasaki, Japan, where he has been engaged in the research and development of dense wavelength-division multiplexing optical transmission systems. From 2000 to 2002, he was with Fujitsu Network Communications, Inc., Richardson, TX. Since 2007, he has also been with Fujitsu Limited, Kawasaki, Japan.

Dr. Hoshida is a member of the Institute of Electronics, Information and Communications Engineers and the Japan Society of Applied Physics.

Jens C. Rasmussen (S'96–M'98) received the Dipl.-Ing. and Dr.-Ing. degrees from Rheinisch-Westfalische Technische Hochschule Aachenm Aachen University, Aachen, Germany, in 1993 and 1998, respectively.

In 1998, he received a scholarship entitled "Two years language and training in Japan" from Deutscher Akademischer AustauschDienst. Since 2000, he has been with Fujitsu Laboratories Ltd., Kawasaki, Japan, where he has been engaged in research and development of dense wavelength-division multiplexing optical transmission systems. Since 2007, he has also been with Fujitsu Ltd., Kawasaki.